Journal of Heat and Mass Transfer Research

Journal homepage: https://jhmtr.semnan.ac.ir

Semnan University

A Novel Electrokinetic Micromixing System with Conductive Mixing-Enclosure-A Geometrical Study

Morteza Nazari[a], Saman Rashidi[*,b], Javad Abolfazli Esfahani[a], Souad Harmand[c]

[a] Department of Mechanical Engineering, Ferdowsi University of Mashhad, Mashhad 91775-1111, Iran.

[b] Department of Energy, Faculty of New Science and Technologies, Semnan University, Semnan, Iran.

[c] Université Polytechnique Hauts-de-France, Laboratoire d'Automatique, de Mécanique et d'Informatique Industrielles et Humaines (LAMIH UMR CNRS 8201), Valenciennes, F59313, France.

PAPER INFO

Paper history:
Received: 2020-11-03
Revised: 2022-06-21
Accepted: 2022-07-16

Keywords:
Electrokinetic micromixer;
Intensification;
Mixing index;
Electric field;
Mixing-enclosure geometry

ABSTRACT

In this paper, an electrokinetic micromixing system with conductive mixing-enclosure is proposed. The simulated micromixer can be fabricated easily and accordingly, it can be used in the microfluidic systems effectively. The mixing process is intensified by controlling the geometry of the mixing-enclosure and electric field strength. The effects of different parameters including existence of mixing-enclosure, horizontal and vertical sizes of mixing-enclosure, orientation angle of mixing-enclosure, and electric field strength on the mixing index are studied. The mixing efficiencies and mixing lengths of current electrokinetic micromixer and those previously proposed by other researchers are compared. The results showed that the mixing efficiency can be enhanced significantly as a micromixer with conductive mixing-enclosure is employed. As an advantage of the proposed micromixer, the maximum mixing efficiency does not change by boosting the electric field strength in the range of 100 $V.cm^{-1}$ to 200 $V.cm^{-1}$, while the mixing time diminishes as the electric field strength increases in this range. For the conductive mixing-enclosure with the orientation angle of 45°, the maximum mixing index of 96.6% is achieved by exerting electric field with strength of 75 $V.cm^{-1}$. The current electrokinetic micromixer has superior mixing efficiency and mixing length as compared with other electrokinetic micromixers.

DOI: 10.22075/jhmtr.2022.21707.1314

1. Introduction

Recently, microfluidic devices are widely used in many applications including chemistry systems [1], biological systems [2], drug delivery process [3, 4], Lab-on-a-chip device [5-8], etc. For most of these applications, providing a fast mixing process is very important [9, 10]. Generally, the Reynolds number has the order of unity or below in the microfluidic modules owing to low values of flow velocity and small characteristic length scale. Accordingly, the flow is laminar and there is no turbulence and fluctuation. In such laminar flow, the mixing process is occurred only by molecular diffusion, which is inherently a slow process [11]. Many active and passive techniques are used to improve the mixing index in the micromixers.

For passive techniques, the external energy sources are not used and the mixing process is completed by the flow influences induced by the geometric features of the micromixer[12, 13]. Cylindrical corrugations [14], parallel and serial lamination [15-17], and flow recombination [18, 19] are some passive techniques used in mixing process. The interface between liquids increases by using the passive techniques and external agitation sources are not used. As a result, the molecular diffusion and chaotic advection are responsible for mixing of species.

Kim et al. [17] designed a novel chaotic passive micromixer. In their micromixer, the chaotic flow generates by periodic perturbing the velocity field created by the periodically placed barriers along the upper wall of the duct. They reported a good mixing

[*] *Corresponding Author: Saman Rashidi*
Email: samanrashidi@semnan.ac.ir

efficiency for their micromixer and the complete mixing can be achieved by using it. In an experimental work, Aoki and Mae [20] investigated the influences of microchannel geometry on the mixing efficiency. The results showed that the mixing efficiency is improved as the flow rate increases or the channel size decreases. Cortes and Tracey [19] used obstacles and grooves inside the mixing duct of a micromixer. They reported that the secondary flows can be generated inside their system, which improves the mixing index of the micromixer. Acoustic [21], thermal influences [22], pressure disturbance [23], magnetic field [24, 25], and electrokinetic [26–31] are some of the active techniques [32–35]. Note that an external source of energy is used in active techniques. As mentioned earlier, the microfluidic systems can be employed in biological applications. However, the temperature of the liquid can be increased by using some active techniques such as thermal or acoustic techniques. This is not suitable for the biological systems because they are very sensitive to the temperature. Moreover, in chemical applications, the reacting liquids may be used, which are sensitive to high temperatures. Tsai and Lin [36] used the thermal bubble micropump to drive the flow and create the oscillatory flow in the micromixer. The oscillatory flow can provide the wavy interface, which increases the contact area and enhances the mixing efficiency. Yaralioglu et al. [21] employed acoustic stirring to provide ultrasonic waves in the micromixer. In their micromixer, the acoustic stirring of the liquid created perpendicular to the main flow direction is responsible for mixing.

Employing the electrokinetic phenomenon is a new active technique used in micromixers. The applications of this phenomenon are not restricted to mixing systems and it has many applications [29,30]. Generally, there MI is no moving components in this technique and it has a very simple structure. In addition, it is suitable for biological systems. In an electrokinetic micromixing system, a number of vortices can be created near the conductive walls that they intensify the mixing process. Rashidi et al. [31] performed a literature review on the electrokinetic mixers. They observed that in most of previous investigations, in this field, investigated the mixing performance when evaluating the effectiveness of electrokinetic mixers. However, mixing time and mixing length are two main factors, which should be investigated because it is important to provide a balance between different parameters. Zhao and Bao [37] employed electrokinetic technique, to provide the mixing in a concentric annulus, as the stirrer. They employed a periodically electric field to induce vortices and chaotic advection in the annulus. The induced vortices and chaotic advection are improved the mixing index in their system. Wu and Li [38] used the conductive hurdles in the microchannels of an electrokinetic micromixer. They employed rectangular, triangular, and circular hurdles and observed that the rectangular hurdle can provide the best mixing performance as compared with triangular and circular hurdles. Azimi et al. [34] installed a conductive flexible plate inside the microchannel of an electrokinetic micromixer. They observed that by exerting the electric field, some vortices can be induced around the plate link, which improve the mixing. In addition, the flexible plate can act as the microstirrer and enhances the mixing process. Recently, Kazemi et al. [35] employed a conductive blade in a microchannel of an electrokinetic Y-shaped micromixer. They found that the throat of the micromixer is best place for plate installation.

In this investigation, a new design of an electrokinetic micromixer is proposed. In this design, a conductive mixing-enclosure is considered for the T-shaped micromixer. The mixing process is intensified by controlling the geometry of the conductive mixing-enclosure and electric field strength. Accordingly, the effects of different parameters, including sizes of mixing-enclosure, orientation angle of mixing-enclosure, and electric field strength, on the mixing index are investigated. This paper is organized by different sections. The physical problem is defined in section 2.

Mathematical modeling including the governing equations, related boundary conditions, and parameters definitions are presented in section 3. The numerical procedure together with the grid independence study and validation results is presented in section 4. The results are reported with their descriptions in section 5. This follows with summarizing the main findings of the paper in conclusion section.

2. Problem Statement

In this research, a T-shaped electrokinetic micromixer with two inlets and one outlet is selected for the simulation. Figure 1 shows the geometry of the micromixing system. As shown in this figure, the horizontal channel of micromixer has width W=100 μm and length L=6W. Moreover, the vertical channel of micromixer has width W and length l=5W. A conductive mixing-enclosure with sides of H×V and angle α is placed near the T-junction. Two liquids flow through the micromixer from entries A and B. One liquid has a sample species with concentration C_0 and other one has not sample species and accordingly, the concentration of zero is considered for this liquid. Three electrodes are located at the inlets and outlet of the system to generate the external electric field. All electrodes have direct connection with the solution. Note that the electroosmotic flow is generated inside the micromixer by the electric field.

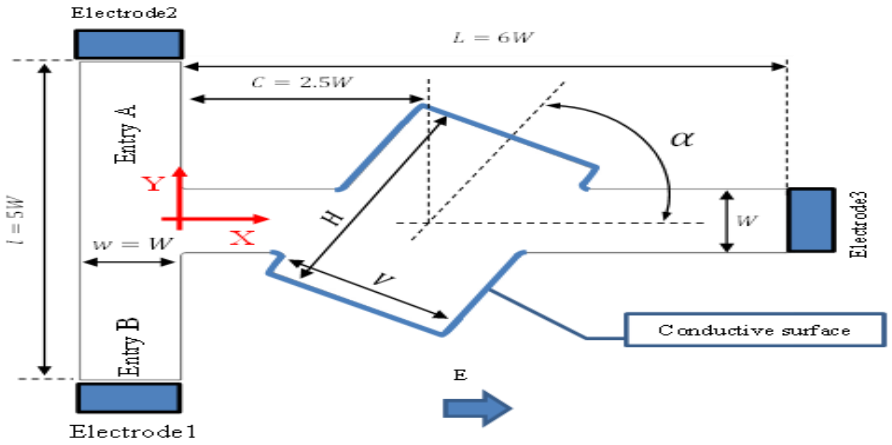

Figure 1. The geometry of the simulated system

The pressure gradient is not considered inside the system and hence the fluid flow is provided by the electroosmosis phenomenon. The zeta potential of -50 mV is considered on the non-conductive surfaces. All values of parameters employed are presented in Table 1. The simulated micromixer has a simple structure and can be fabricated easily. Accordingly, it can be used in the microfluidic systems effectively.

Table 1. Parameters considered in the simulation

Parameters	Value
Dielectric constant, ε	80
Permittivity of vacuum, ε_0 ($CV^{-1}s^{-1}$)	8.854×10^{-12}
Viscosity, μ ($kg\ m^{-1}s^{-1}$)	0.9×10^{-3}
Density, ρ ($kg\ m^{-3}$)	998
Zeta potential of channel wall, ζ_w (mV)	−50
Horizontal channel Width, W (μm)	100
Vertical channel Width, w	W
Horizontal channel Length, L	$6W$
Vertical channel Length, l	$5W$
Diffusion coefficient, D_i (m^2s^{-1})	1.52×10^{-10}
Molar concentration at entry A, C_A($mol\ m^{-3}$)	1
Molar concentration at entry B, C_B ($mol\ m^{-3}$)	0

3. Mathematical Modeling

The following Laplace's equation is solved to determine the electric potential in the micromixer:

$$\nabla^2\vec{\varphi}_e=0 \quad (1)$$

where $\vec{\varphi}_e$ indicates the electric potential. As mentioned before, the walls of the mixing-enclosure are conductive and hence an electric double substrate is formed on them. Note that this substrate can protect the walls from the applied electric field [39, 40]. The boundary conditions for solving this equation are:

Along the channel and mixing-enclosure walls:

$$\vec{n}.\nabla\vec{\varphi}_e=0 \quad (2)$$

Along the inlets of the micromixer:

$$\varphi_e=\varphi_0 \quad (3)$$

Along the outlet of the micromixer:

$$\varphi_e=0 \quad (4)$$

In this study, the incompressible and Newtonian liquid is employed. The following conservation of mass and Navier-Stokes equations are employed:

Conservation of mass equation:

$$\nabla.\vec{u}=0 \quad (5)$$

Navier-Stokes equation:

$$\rho\left[\frac{\partial\vec{u}}{\partial t}+\vec{u}.\nabla\vec{u}\right]=-\nabla\vec{P}+\mu\nabla^2\vec{u}+\vec{E}\rho_e \quad (6)$$

where u, ρ, and μ are velocity, density, and viscosity of the liquid, respectively. Moreover, $\nabla\vec{P}$ and ρ_e indicate the pressure gradient and the local net charge density, respectively. $\vec{E}$= -$\nabla\vec{\varphi}_e$ indicates the local exerted electric field.

Note that in this simulation, the last term placed on the right-hand side of Eq. 6 is neglected as the thickness of electric double substrate is small in most microfluidic systems [41].

The electroosmotic influence is included in the simulation by employing the Helmholtz-Smoluchowski slip velocity. This velocity is:

$$\vec{u}=-\frac{\varepsilon_0\varepsilon\zeta}{\mu}\vec{E} \quad (7)$$

In Eq. 7, ζ_w indicates the zeta potential on the non-conductive wall of the system that a constant value is considered for it. In addition, ζ_i is the induced zeta potential on the conductive walls of the micromixer. The corresponding boundary conditions of these equations are:

At inlet and outlet sections:

$$\vec{n}.\nabla\vec{u}=0 \text{ and } P=P_a \quad (8)$$

On the non-conductive walls:

$$\vec{u}=-\frac{\varepsilon_0\varepsilon\zeta_w}{\mu}\vec{E} \quad (9)$$

On the conductive walls:

$$\vec{u} = -\frac{\varepsilon_0 \varepsilon \zeta_i}{\mu}\vec{E} \quad (10)$$

As mentioned earlier, the pressure gradient is not considered. Accordingly, the following equation is used in the entire flow field:

$$\nabla \vec{P} = 0 \quad (11)$$

The concentration distribution of the electrolyte solution is determined by employing the concentration equation. This equation is:

$$\frac{\partial C}{\partial t} + \nabla(\vec{u}.C - D\nabla C) = 0 \quad (12)$$

In this equation, D and $\vec{C}$ demonstrate the diffusion coefficient and the positional concentration distribution, respectively. Moreover, the boundary conditions of this equation are:

At the entry A:

$$C = C_0 \quad (13)$$

At the entry B:

$$C = 0 \quad (14)$$

On all walls:

$$\frac{\partial C_{t\geq 0}}{\partial n} = 0 \quad (15)$$

Moreover, the initial concentration in the system is:

$$C = 0 \quad (16)$$

3.1. Definition of Efficiency

As discussed in the previous section, two liquids with distinct concentrations flow through the system from entries A and B. The concentrations of them at entries A and B are C_A and C_B, respectively. The mixing index, MI, of the system can be calculated by using the following equation:

$$MI = (1 - \frac{\int_0^W |C - C_\infty| dy}{\int_0^W |C_0 - C_\infty| dy}) \times 100 \quad (16)$$

where C_∞ demonstrates the concentration of ideally mixture, which is calculated by:

$$C_\infty = (C_A + C_B)/2 \quad (17)$$

In addition, C_0 indicates the concentration at entry A. Accordingly, $C_A = C_0$ and $C_B = 0$. Finally, C_i indicates the local concentration at the outlet section.

4. Numerical Simulation

In this study, the MUMPS (Multi-frontal Massively Parallel sparse direct Solver), which is direct finite element solver of COMSOL Multiphysics 5.3a, is employed to solve the set of governing equations as a two-dimensional pressure linked problem. The built-in steady incompressible Navier-Stokes model is employed as the basic model for dealing with the pressure linked equations. Three different physics, namely laminar fluid flow, transports of diluted spices and the electric field, are modeled in this study. The discretization method for laminar flow is P2+P1, which uses the second-order and first-order elements to calculate the velocity the pressure, respectively. Linear and quadratic methods of discretization are employed to solve the concentration and electric field equations.

4.1. Grid Independence Study

An unstructured triangular grid is considered for this problem. A sample view of the grid employed in this study is illustrated in Fig. 2(a). As shown in this figure, a denser grid is used near the sharp corners as compared with other parts for capturing the higher gradients at these regions.

A grid independence study is carried out to insure that the simulation results are independent from the grid sizes. Accordingly, the velocity profile at the cross-section of X=6W, and the concentration distributions at two cross-sections of X=W and X=6W are determined for four grid numbers of 1500, 3000, 6000, and 12000. The results are disclosed in Figs. 2(b), 2(c), and 2(d). It is clear that the percentage differences between the velocity and concentrations calculated by the grid numbers of 6000 and 12000 are very small and hence, the grid number of 6000 is employed for the simulations.

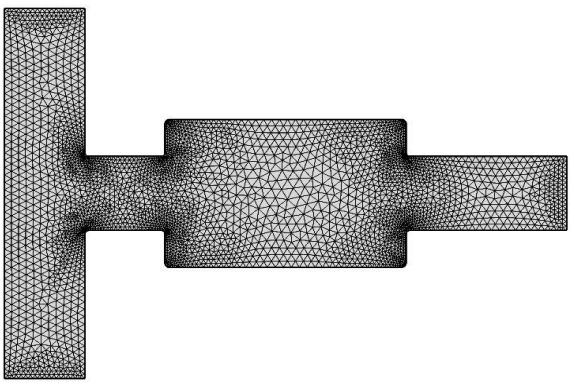

(a)

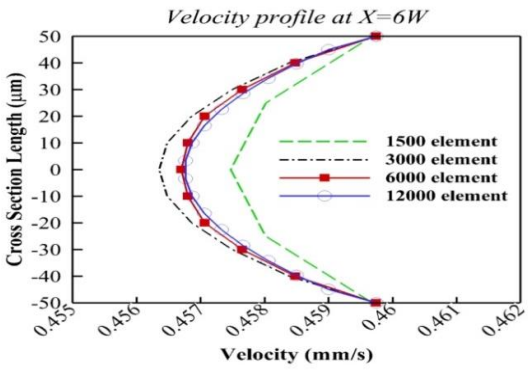

(b)

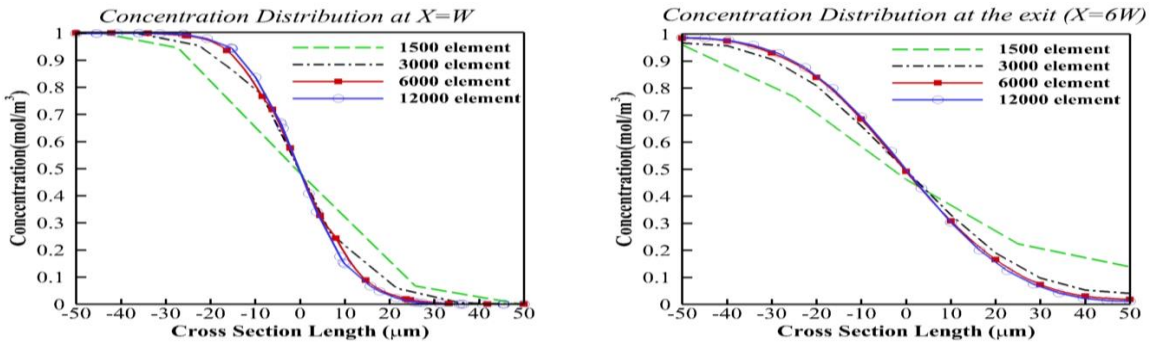

(c) **(d)**

Figure 2. (a) The grid employed in this study; (b) the velocity profile at X=6W; (c) the concentration distribution at X=W; (d) the concentration distribution at X=6

4.2. Validation

To insure about the accuracy of the numerical technique, the results of the present study is compared along with the experimental and numerical results achieved by Wu and Li [38], [41] for a micromixer with two conducting triangle barriers. Figure 3(a) shows the simulated micromixer with the grid used inside it. Figures 3(b) and 3(c) discloses the contour of concentration inside the micromixer and the concentration distributions at the cross section of 0.5 mm after barriers. As shown in these figures, there are good agreements between the numerical results obtained by the present simulation and the data provided by Wu and Li [38], [41].

5. Result and Discussion

The influences of different parameters, including sizes of the mixing-enclosure, mixing-enclosure orientation, and electric field strength, on the MI and concentration distribution in the micromixer are studied.

Figure 4 illustrates the influences of installing a conductive rectangular mixing-enclosure on the MI at E=100 V.cm^{-1}. Three cases are considered in this figure including micromixing system without chamber, micromixing system with non-conductive chamber, and micromixing system with conductive chamber. The contours of concentration distributions of these cases are provided in this figure. The color bars of contours provide the dimensionless concentration distribution. The streamlines are superimposed on these contours. Moreover, the concentration distributions at the outlet for three cases are presented in Fig. 4(d). As illustrated in this figure, for the micromixer without chamber or with non-conductive chamber, as a result of the laminar regime and parallel streamlines, two streams can mix together only at the interface between them by diffusion mechanism that it results in the poor mixing for these cases. For the system with conductive chamber, four vortices are created within the chamber by exerting an electric field. These vortices enhance the mixing between two streams considerably. It should be mentioned that the induced zeta potential can be generated on the conductive wall of the chamber by exerting the external electric field. Induced zeta potential has non constant values and can vary locally on the conductive wall. The mixing efficiencies of 35.18%, 30%, and 84.78% can be achieved by using the micromixing system without chamber, micromixing system with non-conductive chamber, and micromixing system with conductive chamber, respectively. Accordingly, the MI can be enhanced significantly by employing a micromixer with conductive mixing-enclosure.

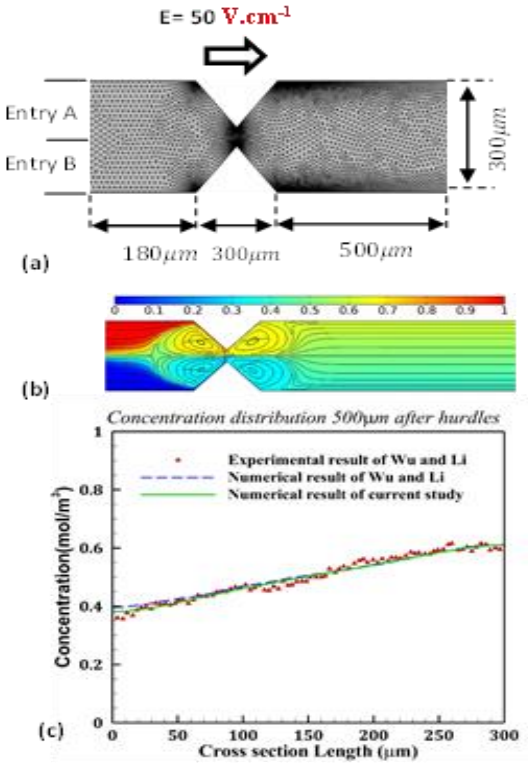

Figure 3. The comparison between the outputs of the present numerical study and the experimental and numerical data achieved by Wu and Li [33]

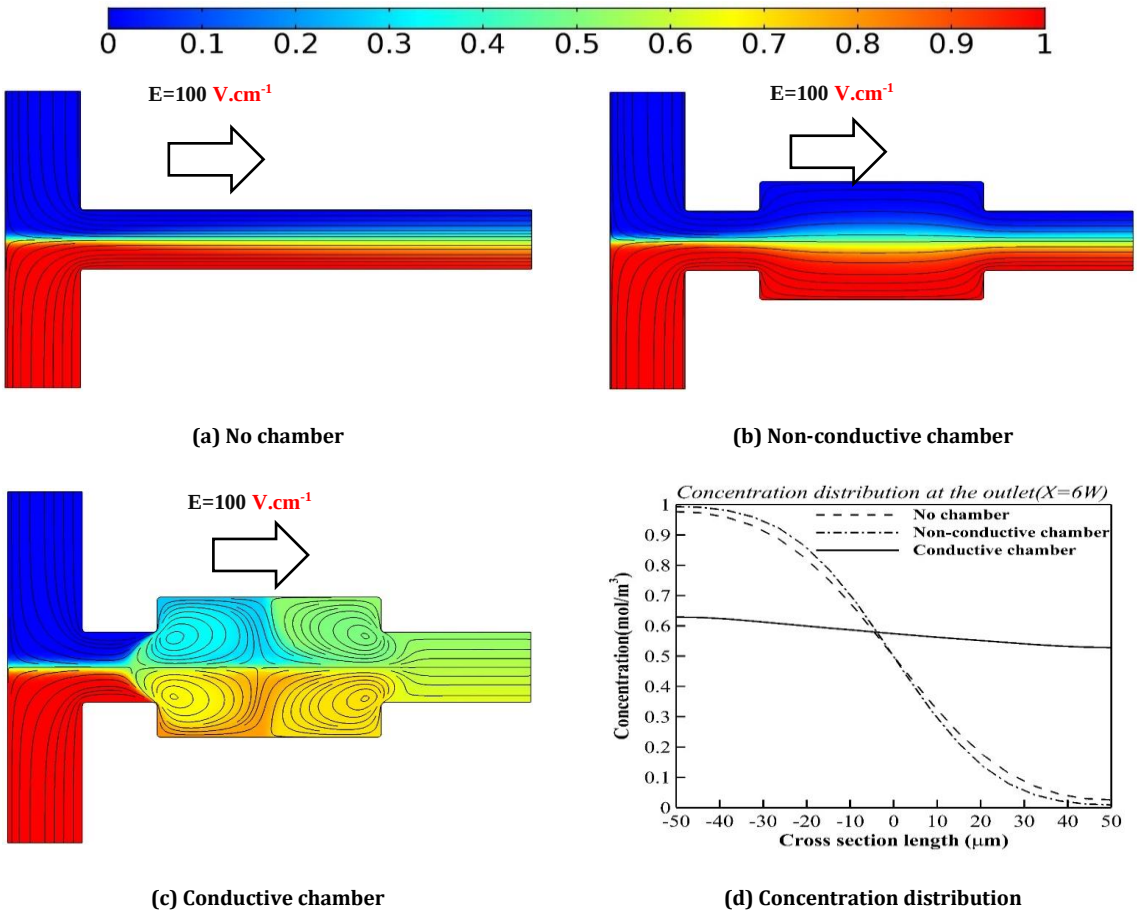

(a) No chamber **(b) Non-conductive chamber**

(c) Conductive chamber **(d) Concentration distribution**

Figure 4. The influences of installing a conductive rectangular mixing-enclosure on the MI at E=100 V.cm^{-1}

Figure 5 displays the influences of mixing-enclosure size on the concentration distribution at E=100 V.cm^{-1}. It can be seen that the sizes of vortices generated inside the mixing-enclosure increases with increasing the vertical and horizontal sizes of the mixing-enclosure. The larger vortices more improve the mixing index in the micromixer. Moreover, it is clear that increasing the horizontal size of the mixing-enclosure is more efficient for improving the mixing index as compared with increasing the vertical size. Note that the vortices elongate along the horizontal direction and more affect the interface between two streams by elongating the mixing-enclosure in horizontal direction. Accordingly, the MI enhances considerably by elongating the mixing-enclosure in horizontal direction. Note that the contact surface between the vortices and interface of two streams increases by increasing the horizontal size of the mixing-enclosure. However, the vortices elongate along the vertical direction and less affect the interface between two streams as the vertical size of the mixing-enclosure increases.

The MI of all cases, investigated in Fig. 5, are presented in Table 2. It is clear that the MI of 84.78% can be achieved by employing a mixing-enclosure with size of H=3W and V=2W.

Table 2. The influences of mixing-enclosure size on the MI at E=100 V.cm^{-1}

H	V	MI (%)
2W	2W	75
3W	2W	84.78
4W	2W	79.73
2W	3W	75.18
2W	4W	71

The influences of conductive mixing-enclosure orientation on flow pattern and concentration distribution at E=100 V.cm^{-1} are displayed in Fig. 6. The symmetry to the centerline of the micromixer is disappeared by changing the orientation angle of the mixing-enclosure (α).

This affects the flow pattern inside the mixing-enclosure. Increasing the orientation angle of the mixing-enclosure up to 45° causes formation of larger vortices in the center of the mixing chamber, which encompass with both liquids. This can increase the contact surface between two liquids and accordingly, the mixing between the two liquids improves.

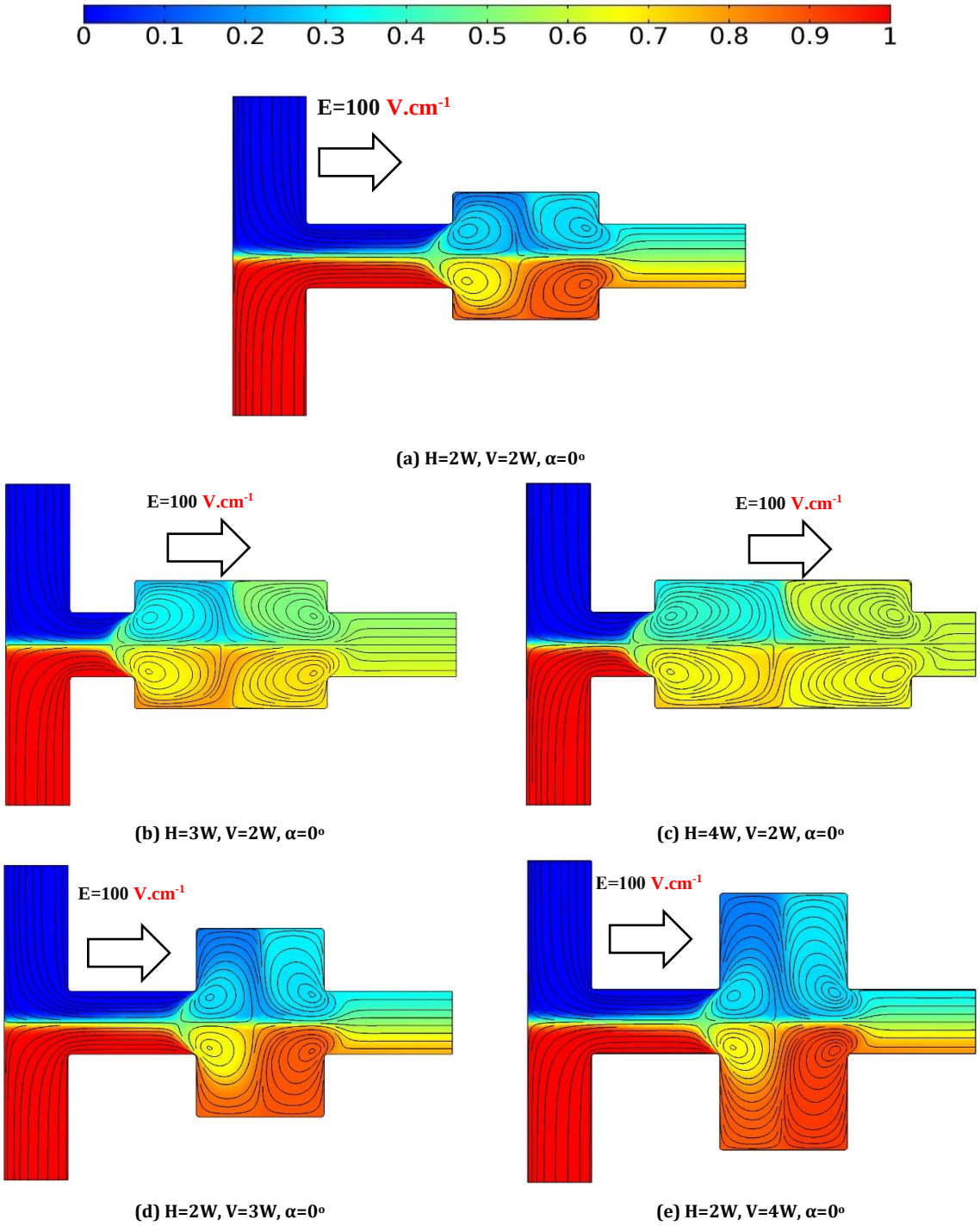

Figure 5. The influences of mixing-enclosure size on the concentration distribution at E=100 V.cm^{-1}

However, for mixing-enclosure with the orientation angle of 0°, two vortices are placed within one liquid and two others are created inside another liquid, which the mixing of two liquids is less for this case. Accordingly, the larger vortices, which occupy whole the mixing-enclosure including both liquids, are created as the orientation angle of the mixing-enclosure increases. This causes an increase in the MI of the micromixer.

The MIs of all cases, considered in Fig. 6, are reported in Table 3. It is clear that the MI improves as the orientation angle of conductive mixing-enclosure is increased. The MI of 99% can be achieved by employing a conductive mixing-enclosure with the orientation angle of 45°. Accordingly, α=45° is the optimum orientation angle of the mixing-enclosure.

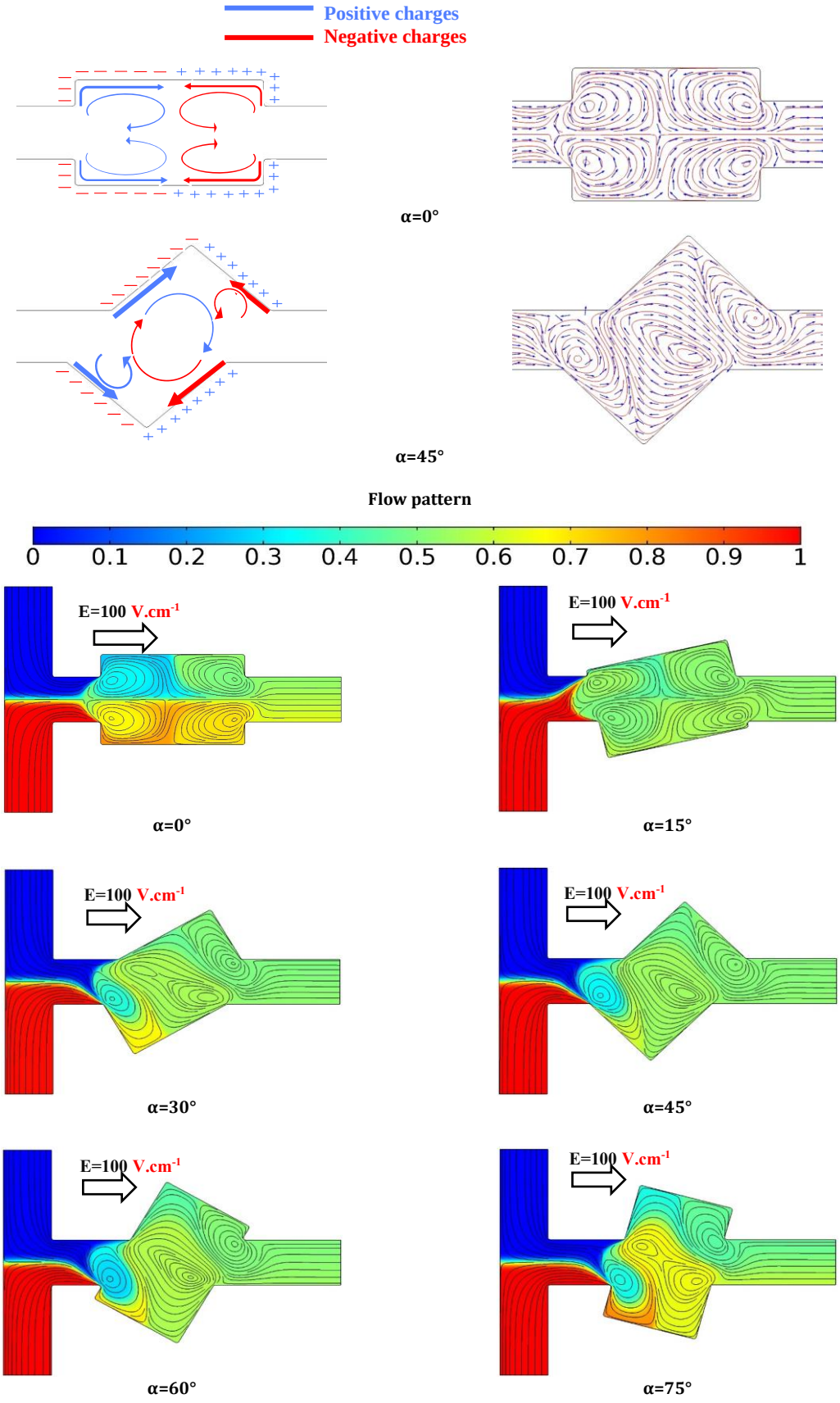

Figure 6. Influences of conductive mixing-enclosure orientation on flow pattern and concentration distribution at E=100 V.cm^{-1}

Table 3. The influences of mixing-enclosure orientation on MI at E=100 V.cm^{-1}

α (deg)	MI (%)
0	84.78
15	93.8
30	96.67
45	99
60	96.3
75	92.9

The influences of electric field strength on the maximum MI and mixing time for α=45° are investigated in Table 4. It should be noted that the case of α=45° is selected for investigation as it is the optimum orientation angle of the mixing-enclosure. Moreover, figure 7 discloses the influences of electric field strength of the concentration distribution for α=45°. In Table 4, the second to sixth columns present the time required to achieve the MI of 1% to 99%. Moreover, the mixing time, reported in this table, is the required time in which the MI changes from 1% to its maximum value for each case. As presented in Table 4, the maximum MIs of 89% and 96.6% can be achieved by exerting the electric field with intensities of 50 V.cm^{-1} and 75 V.cm^{-1}, respectively. The maximum MI does not change as the electric field strength is boosted for E≥100 V.cm^{-1}. However, the mixing time decreases considerably as the electric field strength boosts. For example, the mixing time decreases about 66.40% with boosting the electric field strength in the range of 50 V.cm^{-1} to 200 V.cm^{-1}. Accordingly, as an advantage of the proposed micromixer, the mixing time decreases, while the maximum MI does not change as the electric field strength is boosted beyond 100 V.cm^{-1}. Note that for the micromixers proposed by Wu and Li [41] and Azimi et al. [34], the maximum MI may reduce by booting the electric field strength.

Table 4. The influences of electric field strength on the maximum MI and mixing time for α=45°

E (V.cm^{-1})	MI					Maximum MI (%)	Mixing time (s)
	1%	80%	90%	95%	99%		
	Time (s)						
50	3.3	7.8	-	-	-	89	8.7
75	2.1	5.4	7.3	9.55	-	96.6	9.17
100	1.5	3.9	5.1	6.5	8.2	99	6.7
125	1.2	3.2	4.1	5.1	6.3	99	5.1
150	0.99	2.7	3.6	4.4	5.3	99	4.31
175	0.83	2.3	3	3.6	4.3	99	3.47
200	0.72	2.1	2.6	3.2	3.8	99	3.08

As displayed in Fig. 7, the mixing index improves as the electric field strength boosts in the range of 50 V.cm^{-1} and 75 V.cm^{-1}. However, the mixing index does not change considerbly by increasing the electric field intensities larger than 100 V.cm^{-1}.

Table 5 provides a comparison between the mixing efficiencies and mixing lengths of current electrokinetic micromixer and the electrokinetic micromixers proposed by other researchers. As presented in this table, the current electrokinetic micromixer has better MI and mixing length as compared with other electrokinetic micromixers.

Conclusion

In current paper, the electrokinetic micromixing system with a conductive mixing-enclosure was simulated. The mixing index of the micromixer was improved by controlling the geometry of the conductive mixing-enclosure and changing the electric field strength.

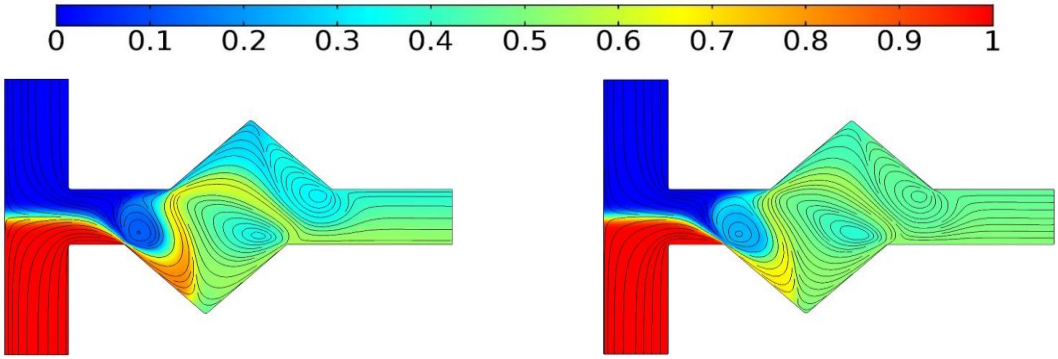

E=50 V.cm^{-1} and t=12s

E=75 V.cm^{-1} and t=11.27s

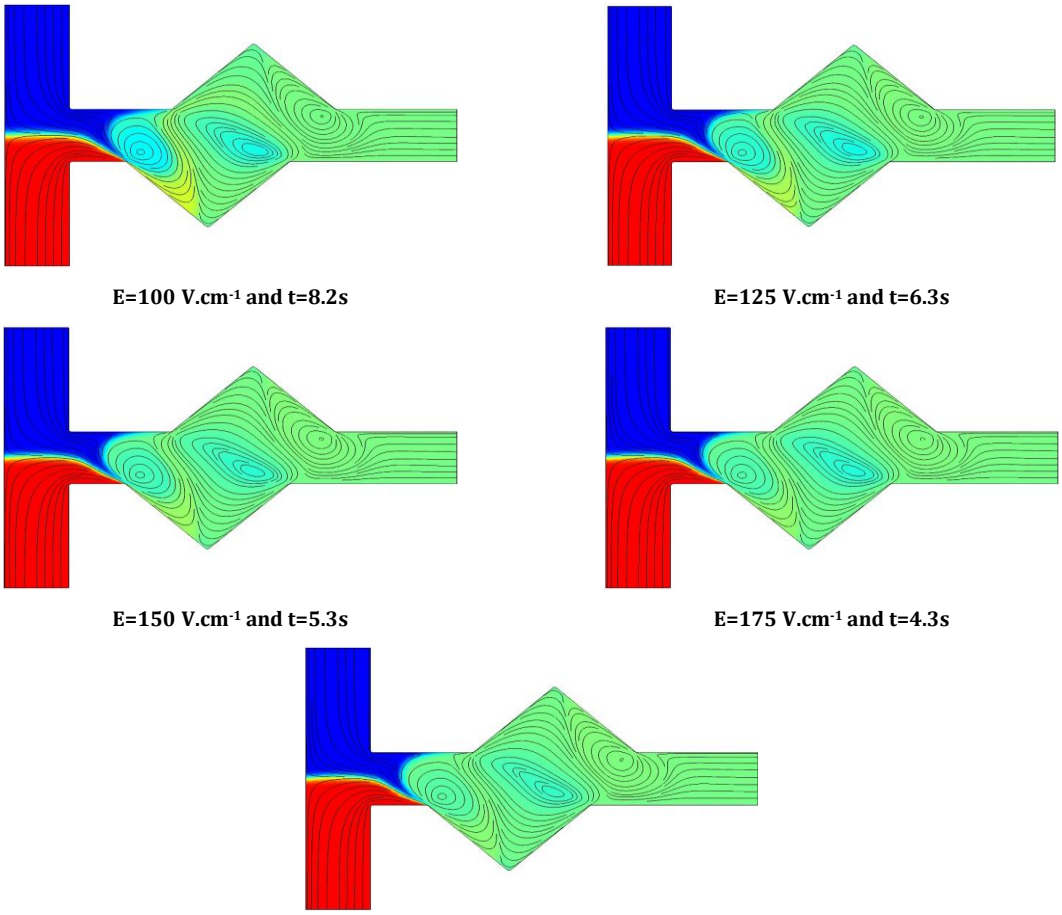

Figure 7. The influences of electric field strength of the concentration distribution for α=45°

Table 5. A comparison between the mixing efficiencies and mixing lengths of current electrokinetic micromixer and the electrokinetic micromixers proposed by other researchers

Study	**Description**	**Applied electrical field, E (V.cm^{-1})**	**Non-dimensional mixing length (Microchannel length/microchannel width)**	MI **(%)**
Wu and Li [33]	Three fully conductive hurdles mounted on the microchannel walls	DC electric field E= 100 V.cm^{-1}	13.3	Using three rectangular conductive hurdles: 94.43% Using three circular conductive hurdles: 91.31% Using three triangular conductive hurdles: 80.26%
Daghighi and Li [37]	One fully conductive spherical particle inside a micro chamber	DC electric field $E_{Horizontal}$ = 40 V.cm^{-1} $E_{Vertical}$ = 40 V.cm^{-1}	10	100%
Azimi el al. [34]	One fully conductive flexible link connected to the upper wall of a straight microchannel	time-varying DC electric field $E_{average}$ = 50 V.cm^{-1}	20	90%
Current study	One rectangular conductive mixing-enclosure at α = 45	DC electric field E= 100 V.cm^{-1}	6	99%

The effects of different parameters including existence of conductive mixing-enclosure, horizontal and vertical sizes of mixing-enclosure, orientation angle of mixing-enclosure, and electric field strength on the MI in this micromixer were investigated. The important results of current study are:

- The MI can be enhanced significantly by using a micromixer with conductive mixing-enclosure.
- The mixing efficiencies of 35.18%, 30%, and 84.78% can be achieved by employing the micromixing system without chamber, micromixing system with non-conductive chamber, and micromixing system with conductive chamber, respectively.
- Increasing the horizontal size of the mixing-enclosure is more efficient for improving the MI as compared with increasing the vertical size.
- The maximum MI is occurred at the orientation angle of 45°.
- For the conductive mixing-enclosure with the orientation angle of 45°, the maximum MIs of 89% and 96.6% can be achieved by exerting the electric field with intensities of 50 $V.cm^{-1}$ and 75 $V.cm^{-1}$, respectively. The maximum MI does not change by increasing the electric field strength for $E \geq 100$ $V.cm^{-1}$.
- As an advantage of the proposed micromixer, the MI does not change by boosting the electric field strength from 100 $V.cm^{-1}$ to 200 $V.cm^{-1}$, while the mixing time decreases as the electric field strength is increased in this range. Accordingly, it is possible to diminish the mixing time with keeping the high MI of the micromixer.
- The current electrokinetic micromixer has better MI and mixing length as compared with other electrokinetic micromixers.

References

[1] Demello, A.J., 2006. Control and detection of chemical reactions in microfluidic systems. *Nature*, *442*(7101), pp.394-402.

[2] Meagher, R.J., Hatch, A.V., Renzi, R.F. and Singh, A.K., 2008. An integrated microfluidic platform for sensitive and rapid detection of biological toxins. *Lab on a Chip*, *8*(12), pp.2046-2053.

[3] Khetani, S.R. and Bhatia, S.N., 2008. Microscale culture of human liver cells for drug development. *Nature biotechnology*, *26*(1), pp.120-126.

[4] Dittrich, P.S. and Manz, A., 2006. Lab-on-a-chip: microfluidics in drug discovery. *Nature reviews Drug discovery*, *5*(3), pp.210-218.

[5] Anderson, R.C., Su, X., Bogdan, G.J. and Fenton, J., 2000. A miniature integrated device for automated multistep genetic assays. *Nucleic acids research*, *28*(12), pp.e60-e60.

[6] Bayareh, M., Ashani, M.N. and Usefian, A., 2020. Active and passive micromixers: A comprehensive review. *Chemical Engineering and Processing-Process Intensification*, *147*, p.107771.

[7] Bayareh, M., Usefian, A. and Ahmadi Nadooshan, A., 2019. Rapid mixing of Newtonian and non-Newtonian fluids in a three-dimensional micro-mixer using non-uniform magnetic field. *Journal of Heat and Mass Transfer Research*, *6*(1), pp.55-61.

[8] Usefian, A. and Bayareh, M., 2020. Numerical and experimental investigation of an efficient convergent–divergent micromixer. *Meccanica*, *55*(5), pp.1025-1035.

[9] Kang, D. K., et al., 2014. Rapid detection of single bacteria in unprocessed blood using Integrated Comprehensive Droplet Digital Detection. *Nature Communications*, vol. 5, pp. 1–10.

[10] Nguyen, D.P., Kloosterman, F., Barbieri, R., Brown, E.N., Wilson, M.A. and Klausberger, T., 2005. Z.: Micromixers–a review. In *Journal of Micromechanics and Microengineering*.

[11] Jahn, A., Stavis, S.M., Hong, J.S., Vreeland, W.N., DeVoe, D.L. and Gaitan, M., 2010. Microfluidic mixing and the formation of nanoscale lipid vesicles. *ACS nano*, *4*(4), pp.2077-2087.

[12] Baheri Islami, S., Khezerloo, M. and Gharraei, R., 2017. The effect of chaotic advection on mixing degree and pressure drop of non-Newtonian fluids flow in curved micromixers. *Journal of the Brazilian Society of Mechanical Sciences and Engineering*, *39*(3), pp.813-831.

[13] Zhang, S. and Chen, X., 2018. A novel passive micromixer based on Koch fractal principle. *Journal of the Brazilian Society of Mechanical Sciences and Engineering*, *40*(10), pp.1-9.

[14] Stroock, A.D., Dertinger, S.K., Ajdari, A., Mezic, I., Stone, H.A. and Whitesides, G.M., 2002. Chaotic mixer for microchannels. *Science*, *295*(5555), pp.647-651.

[15] Gray, B.L., Jaeggi, D., Mourlas, N.J., Van Drieenhuizen, B.P., Williams, K.R., Maluf, N.I. and Kovacs, G.T.A., 1999. Novel interconnection technologies for integrated microfluidic systems. *Sensors and Actuators A: Physical*, *77*(1), pp.57-65.

[16] Yi, M. and Bau, H.H., 2003. The kinematics of bend-induced mixing in micro-conduits. *International Journal of Heat and Fluid Flow*, *24*(5), pp.645-656.

[17] Ismagilov, R.F., Stroock, A.D., Kenis, P.J., Whitesides, G. and Stone, H.A., 2000. Experimental and theoretical scaling laws for transverse diffusive broadening in two-phase laminar flows in microchannels. *Applied Physics Letters*, *76*(17), pp.2376-2378.

[18] Chen, X., Li, T., Zeng, H., Hu, Z. and Fu, B., 2016. Numerical and experimental investigation on micromixers with serpentine microchannels. *International Journal of Heat and Mass Transfer*, *98*, pp.131-140.

[19] Lee, C.Y., Wang, W.T., Liu, C.C. and Fu, L.M., 2016. Passive mixers in microfluidic systems: A review. *Chemical Engineering Journal*, *288*, pp.146-160.

[20] Aoki, N. and Mae, K., 2006. Effects of channel geometry on mixing performance of micromixers using collision of fluid segments. *Chemical Engineering Journal*, *118*(3), pp.189-197.

[21] Yaralioglu, G.G., Wygant, I.O., Marentis, T.C. and Khuri-Yakub, B.T., 2004. Ultrasonic mixing in microfluidic channels using integrated transducers. *Analytical chemistry*, *76*(13), pp.3694-3698.

[22] Mao, H., Yang, T. and Cremer, P.S., 2002. A microfluidic device with a linear temperature gradient for parallel and combinatorial measurements. *Journal of the American Chemical Society*, *124*(16), pp.4432-4435.
[23] Ma, Y., Sun, C.P., Fields, M., Li, Y., Haake, D.A., Churchill, B.M. and Ho, C.M., 2008. An unsteady microfluidic T-form mixer perturbed by hydrodynamic pressure. *Journal of Micromechanics and Microengineering*, *18*(4), p.045015.
[24] Lu, L.H., Ryu, K.S. and Liu, C., 2002. A magnetic microstirrer and array for microfluidic mixing. *Journal of microelectromechanical systems*, *11*(5), pp.462-469.
[25] Suzuki, H. and Ho, C.M., 2002, January. A magnetic force driven chaotic micro-mixer. In *Technical Digest. MEMS 2002 IEEE International Conference. Fifteenth IEEE International Conference on Micro Electro Mechanical Systems (Cat. No. 02CH37266)* (pp. 40-43). IEEE.
[26] Nazari, M., Rashidi, S. and Esfahani, J.A., 2020. Effects of flexibility of conductive plate on efficiency of an induced-charge electrokinetic micro-mixer under constant and time-varying electric fields-a comprehensive parametric study. *Chemical Engineering Science*, *212*, p.115335.
[27] Nazari, M., Chuang, P.Y.A., Esfahani, J.A. and Rashidi, S., 2020. A comprehensive geometrical study on an induced-charge electrokinetic micromixer equipped with electrically conductive plates. *International Journal of Heat and Mass Transfer*, *146*, p.118892.
[28] Azimi, S., Nazari, M. and Daghighi, Y., 2016. Fluid physics around conductive deformable flaps within an induced-charge electrokinetically driven microsystem. *Microfluidics and Nanofluidics*, *20*(9), pp.1-16.
[29] Azimi, S., Nazari, M. and Daghighi, Y., 2017. Developing a fast and tunable micro-mixer using induced vortices around a conductive flexible link. *Physics of Fluids*, *29*(3), p.032004.
[30] Daghighi, Y., Gao, Y. and Li, D., 2011. 3D numerical study of induced-charge electrokinetic motion of heterogeneous particle in a microchannel. *Electrochimica acta*, *56*(11), pp.4254-4262.
[31] Daghighi, Y. and Li, D., 2013. Numerical study of a novel induced-charge electrokinetic micro-mixer. *Analytica chimica acta*, *763*, pp.28-37.
[32] Usefian, A., Bayareh, M., Shateri, A. and Taheri, N., 2019. Numerical study of electro-osmotic micro-mixing of Newtonian and non-Newtonian fluids. *Journal of the Brazilian Society of Mechanical Sciences and Engineering*, *41*(5), pp.1-10.
[33] Usefian, A. and Bayareh, M., 2019. Numerical and experimental study on mixing performance of a novel electro-osmotic micro-mixer. *Meccanica*, *54*(8), pp.1149-1162.
[34] Saha, S., Gopmandal, P.P. and Ohshima, H., 2019. Electroosmotic flow and transport of ionic species through a slit soft nanochannel filled with general electrolytes. *Meccanica*, *54*(14), pp.2131-2149.
[35] Qi, C. and Ng, C.O., 2018. Rotating electroosmotic flow in a non-uniform microchannel. *Meccanica*, *53*(8), pp.2105-2120.
[36] Tsai, J.H. and Lin, L., 2002. Active microfluidic mixer and gas bubble filter driven by thermal bubble micropump. *Sensors and Actuators A: Physical*, *97*, pp.665-671.
[37] Zhao, H. and Bau, H.H., 2007. Microfluidic chaotic stirrer utilizing induced-charge electro-osmosis. *Physical Review E*, *75*(6), p.066217.
[38] Wu, Z. and Li, D., 2008. Micromixing using induced-charge electrokinetic flow. *Electrochimica Acta*, *53*(19), pp.5827-5835.
[39] Helmholtz, H., Der phystk und chemie. 1. no. 2, 1853.
[40] Dukhin, A.S. and Goetz, P.J., 2010. Fundamentals of interface and colloid science. In *Studies in Interface Science* (Vol. 24, pp. 21-89). Elsevier.
[41] Wu, Z. and Li, D., 2008. Mixing and flow regulating by induced-charge electrokinetic flow in a microchannel with a pair of conducting triangle hurdles. *Microfluidics and nanofluidics*, *5*(1), pp.65-76.